Asparagine and glutamine ladders promote cross-species prion conversion

Received for publication, May 1, 2017, and in revised form, September 1, 2017 Published, Papers in Press, September 20, 2017, DOI 10.1074/jbc.M117.794107

Timothy D. Kurt[‡1], Patricia Aguilar-Calvo[‡1], Lin Jiang[‖], José A. Rodriguez[§¶‡‡], Nazilla Alderson[‡], David S. Eisenberg[§¶], and Christina J. Sigurdson[‡2]**

*From the [‡]Departments of Pathology and Medicine, University of California at San Diego, La Jolla, California 92093, the [§]UCLA-DOE Institute, Howard Hughes Medical Institute, Los Angeles, California 90095, the [¶]Molecular Biology Institute, [‡‡]the Department of Chemistry and Biochemistry, and the [‖]Department of Neurology, UCLA, Los Angeles, California 90095, and the **Department of Pathology, Immunology, and Microbiology, University of California at Davis, Davis, California 95616*

Edited by Paul E. Fraser

Prion transmission between species is governed in part by primary sequence similarity between the infectious prion aggregate, PrP^{Sc}, and the cellular prion protein of the host, PrP^{C}. A puzzling feature of prion formation is that certain PrP^{C} sequences, such as that of bank vole, can be converted by a remarkably broad array of different mammalian prions, whereas others, such as rabbit, show robust resistance to cross-species prion conversion. To examine the structural determinants that confer susceptibility or resistance to prion conversion, we systematically tested over 40 PrP^{C} variants of susceptible and resistant PrP^{C} sequences in a prion conversion assay. Five key residue positions markedly impacted prion conversion, four of which were in steric zipper segments where side chains from amino acids tightly interdigitate in a dry interface. Strikingly, all five residue substitutions modulating prion conversion involved the gain or loss of an asparagine or glutamine residue. For two of the four positions, Asn and Gln residues were not interchangeable, revealing a strict requirement for either an Asn or Gln residue. Bank voles have a high number of Asn and Gln residues and a high Asn:Gln ratio. These findings suggest that a high number of Asn and Gln residues at specific positions may stabilize β-sheets and lower the energy barrier for cross-species prion transmission, potentially because of hydrogen bond networks from side chain amides forming extended Asn/Gln ladders. These data also suggest that multiple PrP^{C} segments containing Asn/Gln residues may act in concert along a replicative interface to promote prion conversion.

Prion diseases are fatal neurodegenerative disorders of humans and animals caused by prion protein aggregates accumulating in the brain and spinal cord (1). β-Sheet–rich prion aggregates, known as PrP^{Sc}, template the misfolding of the cellular prion protein monomer, PrP^{C}, similar to seeding mechanisms that occur with other amyloidogenic proteins such as amyloid-β, α-synuclein, and islet amyloid polypeptide (2, 3). PrP^{Sc}-templated conversion of PrP^{C} monomers typically requires a high degree of sequence similarity (4–6); however, conversion of dissimilar PrP sequences can occur and induce prion disease in other species; for example, bovine spongiform encephalopathy prions have infected humans, cats, and zoo bovids (7, 8).

Mammalian PrP^{C} is highly conserved in both sequence and structure, consisting of ~210 amino acids with a disordered N terminus (residues 23–120) and a globular, C-terminal domain arranged as three α-helices and a short anti-parallel β-sheet (9, 10). We found that conversion of mouse or human PrP^{C} by elk chronic wasting disease (CWD)[3] prions occurs efficiently when the PrP^{C} sequence within a loop segment rich in polar and aromatic residues, the $\beta2$–$\alpha2$ loop, is mutated to match the elk sequence (VDQYNNQNTF) (11, 12). Further studies of the $\beta2$–$\alpha2$ loop sequence revealed that substituting Tyr^{169} with glycine, leucine, or glutamine inhibited prion conversion, whereas substitutions of bulky aromatic residues (Y169W and Y169F) enabled conversion, indicating a requirement for highly specific amino acid side chain properties, in this case, an aromatic side chain (13). Collectively, these findings suggest that prion conversion between different PrP sequences does not require an exact match in the side chain between PrP^{C} and PrP^{Sc}; however, side chain complementarity in amyloid-prone segments is essential. The $\beta2$–$\alpha2$ loop has been identified as a steric zipper segment of PrP, in which side chains emerging from two β-sheets tightly interdigitate, forming a dry interface (14). Although residue mismatches between species may diminish steric zipper formation, polar, hydrophobic, and aromatic residues in steric zipper segments may also stabilize early aggregates via aromatic residue stacks, serine stacks, and asparagine ladders and thus may promote conversion to a β-sheet–rich isoform (15, 16)

The bank vole is a rodent that has proven remarkably susceptible to a diverse array of prions from humans and animals, and bank vole PrP^{C} has recently been termed the "universal accep-

This work was supported by National Institutes of Health grants NS069566 (to C. J. S.), NS076896 (to C. J. S.), OD019919 (to T. D. K.), and OD017853 (to T. D. K.). The authors declare that they have no conflicts of interest with the contents of this article. The content is solely the responsibility of the authors and does not necessarily represent the official views of the National Institutes of Health.
This article contains supplemental Figs. S1 and S2.

[1] Both authors contributed equally to this work.

[2] To whom correspondence should be addressed: Dept. of Pathology, UC San Diego, 9500 Gilman Dr., La Jolla, CA 92093-0612. Tel.: 858-534-0978; Fax: 858-246-0523; E-mail: csigurdson@ucsd.edu.

[3] The abbreviations used are: CWD, chronic wasting disease; PMCA, protein misfolding cyclic amplification; clPMCA, cell-lysate PMCA; PK, proteinase K; Hu, human; Bv, bank vole; Rb, rabbit; ANOVA, analysis of variance; RML, Rocky Mountain Laboratory.

tor" sequence (17–21). In contrast, other PrP^C sequences, such as that of rabbit, are more resistant to seeded conversion by prions from another species or cross-seeded conversion (22). Notably, certain residues in the bank vole and rabbit were identified as influencing seeded prion conversion (22–25). Yet in general the residues and underlying mechanisms controlling cross-species prion conversion are unclear. Here we used PrP^C sequences from susceptible and resistant species in an *in vitro* prion conversion assay, cell-lysate protein misfolding cyclic amplification (clPMCA) (12, 13, 26), to identify the key residue positions that promote or inhibit prion conversion. We systematically substituted single residues in bank vole, rabbit, and human PrP^C and seeded with dissimilar elk or mouse prions to examine the mechanism of prion conversion. Conversion of three mammalian PrP^C sequences with single or multiple substitutions has revealed Asn/Gln residues in PrP, often within known steric zippers, as powerful promoters of prion conversion among dissimilar sequences, suggesting that within a β-sheet, the linear chains of hydrogen bonds among the amides in Asn/Gln side chains stabilize and enhance prion assembly.

Results

Replacing asparagine and glutamine residues in bank vole PrP^C inhibits its conversion

The amino acid sequences of bank vole, rabbit, and human PrP^C differ at 27 positions in fully processed PrP (Fig. 1*A*), yet show highly similar secondary and tertiary structure by NMR spectroscopy (27–29). To identify the residues that impact prion cross-seeding, we first compared the conversion of bank vole, human, and rabbit PrP^C seeded by elk and mouse prions. The two mouse prions used, RML and 87V, differ in amino acid sequence in two positions (supplemental Fig. S1) and in the PrP^{Sc} biochemical properties and disease phenotype in mice (30). Each PrP^C sequence was expressed in PrP-deficient RK13 cells, and cell lysates were seeded with prions or were unseeded (supplemental Fig. S2) and subjected to clPMCA. Samples were then analyzed for proteinase K (PK)–resistant PrP^{Sc} by Western blotting, using the anti-PrP 3F4 antibody epitope for detection of newly converted PrP^{Sc} (31). Bank vole PrP^C ($BvPrP^C$) was readily seeded by elk CWD as well as mouse 87V and RML prions, whereas human ($HuPrP^C$) and rabbit PrP^C ($RbPrP^C$) were not converted by any of the prions (Fig. 1*B*), confirming that the conversion efficiency reported for $BvPrP^C$, $HuPrP^C$, and $RbPrP^C$ (32–35) could be reproduced in the clPMCA assay.

To identify the $HuPrP^C$ residues that obstruct prion conversion, bank vole PrP^C with human residue substitutions was used as a substrate in clPMCA (Fig. 1*C*). Fifteen residue substitutions were tested singly or grouped (positions 227–229) (Fig. 1*A*), five of which had a major effect on conversion. $BvPrP^C$ with the V166M or Q168E substitutions from $HuPrP^C$ ($\beta2$–$\alpha2$ loop) markedly reduced conversion when seeded with mouse RML, mouse 87V, or elk CWD (~10–50% conversion relative to $BvPrP^C$) (Fig. 1, *D* and *E*). The N143S substitution ($\beta1$–$\alpha1$ loop) was strongly inhibitory for RML and 87V mouse prions (14 and 7% conversion, respectively), but not CWD (>100% conversion) (Fig. 1, *D* and *E*). Additionally, N155H was inhibitory for 87V-induced conversion (47% conversion), and Q219E was inhibitory for RML-induced conversion (20% conversion) (Fig. 1, *D* and *E*). Given that all three PrP^{Sc} sequences include Asn^{143} and Gln^{219} (supplemental Fig. S1), successful conversion is not likely due simply to a primary sequence match with PrP^C but instead was influenced by the PrP^{Sc} conformation. $BvPrP^C$ with 10 other human residue substitutions was converted to high PrP^{Sc} levels by all three prions (Fig. 1, *D* and *E*), indicating that most human residues do not inhibit cross-seeding by CWD or certain mouse prions. Thus, substitution of two human PrP^C residues (Met^{166} and Glu^{168}) inhibited conversion of $BvPrP^C$ by all prions tested, and three other substitutions (Ser^{143}, His^{155}, Glu^{219}) inhibited prion conversion to 50% or less in a PrP^{Sc} sequence- and/or conformation-specific manner.

Rabbits have resisted intracerebral challenge with Creutzfeldt–Jakob disease, kuru, sheep scrapie, and mouse-adapted scrapie prions (strain ME7) (32, 33), and are considered one of the most highly prion-resistant species. We next measured the conversion of $BvPrP^C$ having nine single or grouped rabbit-specific residue substitutions (Fig. 1*C*). The N100G substitution showed the most dramatic inhibition, with ≤10% conversion, whereas K220Q resulted in only 37–57% conversion by any prion (Fig. 1, *F* and *G*). The M138L, I184V, and M205I rabbit substitutions reduced CWD-seeded conversion to ~30, 40, and 25% conversion, respectively (Fig. 1, *F* and *G*). Additionally, N174S completely blocked mouse 87V-seeded conversion of $BvPrP^C$ but only reduced RML-seeded conversion to ~40% (Fig. 1, *F* and *G*). Thus, six of nine rabbit substitutions diminished conversion of bank vole PrP^C by more than 50%. Collectively, these results demonstrate that human and rabbit residues impede prion conversion to varying levels, depending on the PrP^{Sc} sequence and/or conformation. Remarkably, the five most inhibitory substitutions, N100G, N143S, Q168E, N174S, and Q219E, involved the loss of an asparagine or glutamine residue from the bank vole sequence, suggesting that Asn/Gln residues are important for the conversion of bank vole PrP.

Bank vole asparagine and glutamine residues enable prion conversion of human and rabbit PrP^C

Because the N100G, N143S, Q168E, N174S, and Q219E substitutions inhibited conversion of $BvPrP^C$, we reasoned that the converse bank vole amino acid substitutions may enable prion conversion of otherwise resistant $HuPrP^C$ and $RbPrP^C$ (Fig. 2*A*). We measured seeded conversion of $HuPrP^C$ having the S143N, E168Q, or E219Q substitutions and $RbPrP^C$ containing the G100N or S174N substitutions. $HuPrP^C$ with the S143N or E168Q substitutions seeded with 87V or CWD prions, respectively, led to low PrP^{Sc} levels (Fig. 2, *B* and *C*), whereas E219Q had no effect on conversion (Fig. 2, *B* and *C*). In contrast, mouse RML prions did not convert any of the $HuPrP^C$ sequences with single substitutions (Fig. 2, *B* and *C*). To identify any other residues that impact cross-seeding of $HuPrP^C$, we assessed 12 other Hu-to-Bv amino acid substitutions including the adjacent residues 219–220 and 227–229. Only the Q168E and S170N substitutions in $HuPrP^C$ resulted in modest conversion when seeded by CWD prions (Fig. 2, *B* and *C*), as previously reported (12), whereas no other substitution enabled conversion by mouse RML or 87V prions.

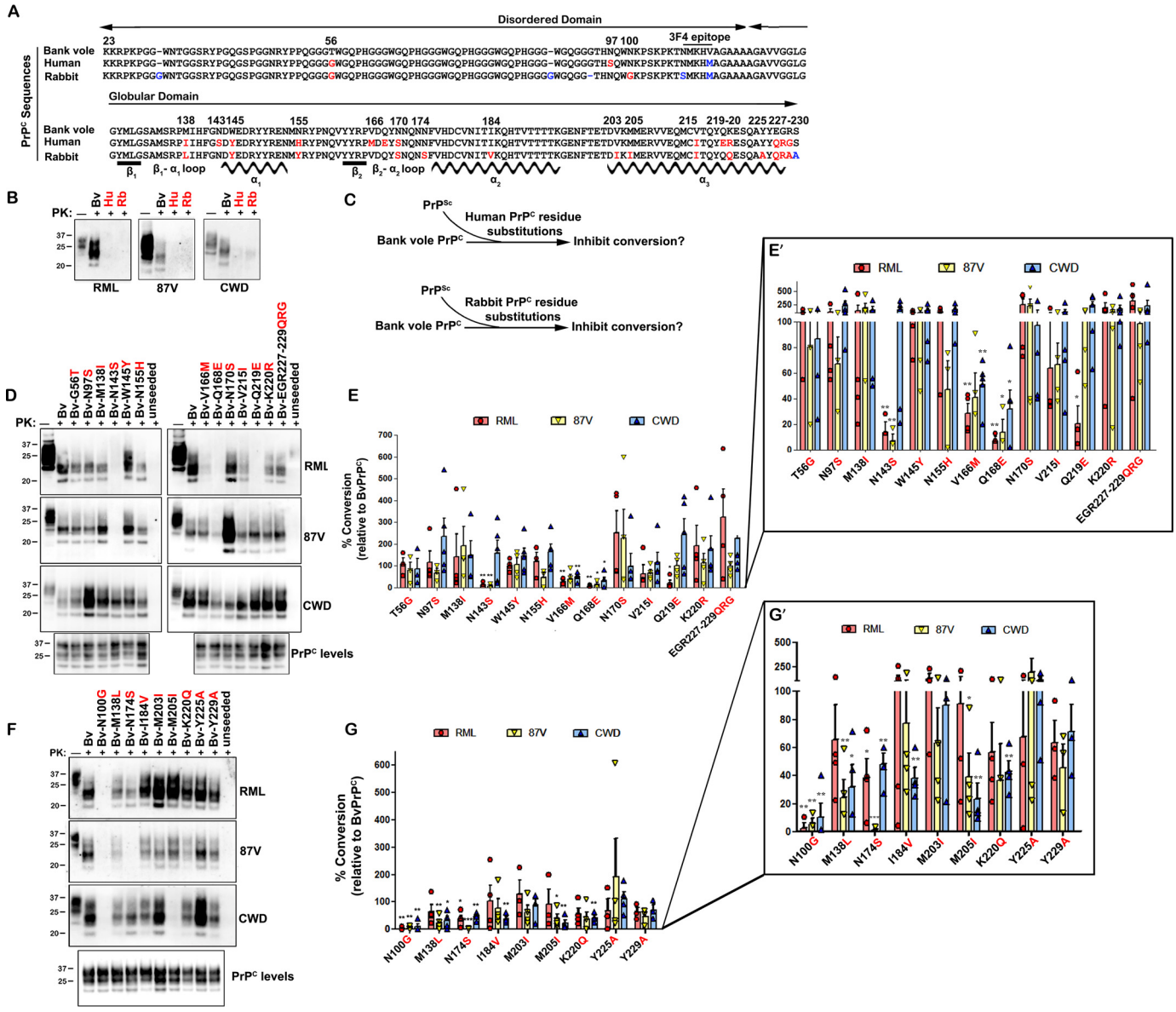

Figure 1. Human and rabbit amino acid substitutions inhibit conversion of bank vole PrP^C. *A*, alignment of the PrP^C sequences from bank vole, human, and rabbit reveals amino acid sequence differences between species at 27 positions (labeled in *red* and *blue*), 21 of which were investigated here (in *red*). Locations of the β-strands and α-helices are shown. *B*, mouse RML, mouse 87V, and elk CWD prions convert bank vole BvPrP^C, but not HuPrP^C or RbPrP^C. *C*, schematic for experimental approach. BvPrP^C with HuPrP^C or RbPrP^C substitutions was seeded with mouse or elk prions, and the newly converted PrP^{Sc} was measured after 24 h. *D*, representative immunoblots show conversion of BvPrP^C with amino acid substitutions from HuPrP^C. *E*, quantitative analysis shows that substitutions N143S, Q168E, and Q219E strongly inhibit BvPrP^C conversion, depending on the PrP^{Sc} seed. *F*, representative immunoblots show conversion of BvPrP^C with amino acid substitutions from RbPrP^C. *G*, quantitative analysis shows that the N100G and N174S substitutions strongly inhibit conversion, depending on the PrP^{Sc} seed. *E′* and *G′* show the quantified data with a segmented *y* axis. For *A*, the GenBank^{TM} accession numbers for bank vole, human, and rabbit PrP^C are AF367624, DQ408531, and U28334, respectively. Quantified data are from three to five independent experiments (*E* and *G*). The *error bars* indicate the observed variance. *, $p < 0.05$; **, $p < 0.01$; ***, $p < 0.001$, one-sample *t* test. One-way ANOVA with Tukey post hoc test revealed statistically significant differences for CWD between residue substitutions at positions 100 and 203, positions 138 and 225, and positions 205 and 225 (*, $p < 0.05$), as well as between residues 100 and 225 (**, $p < 0.01$).

We next measured conversion of RbPrP^C with the bank vole substitutions G100N or S174N. Remarkably, the single G100N substitution resulted in efficient cross-seeding by CWD, 87V, and RML prions (>100, 84, and 83%, respectively) (Fig. 2, *D* and *E*), indicating that the Asn^{100} residue is critical for conversion by all three prions. The single S174N substitution had minimal impact on conversion by RML, 87V, and CWD prions (4, 41, and 43%, of BvPrP^C, respectively) (Fig. 2, *D* and *E*), whereas RbPrP^C containing both G100N and S174N was converted to levels similar to RbPrP^C containing the single G100N substitution (Fig. 2, *D* and *E*). These results suggest that certain asparagine and glutamine residues in BvPrP^C (Asn^{100}, Asn^{143}, Gln^{168}, Asn^{170}) promote cross-species prion conversion, even in the context of a different PrP sequence.

Bank vole substitutions variably promote conversion of human PrP^C in a prion-dependent manner

Because no single BvPrP substitution enabled conversion of HuPrP^C by more than 50%, we next assessed conversion of HuPrP^C having multiple substitutions. HuPrP^C with the com-

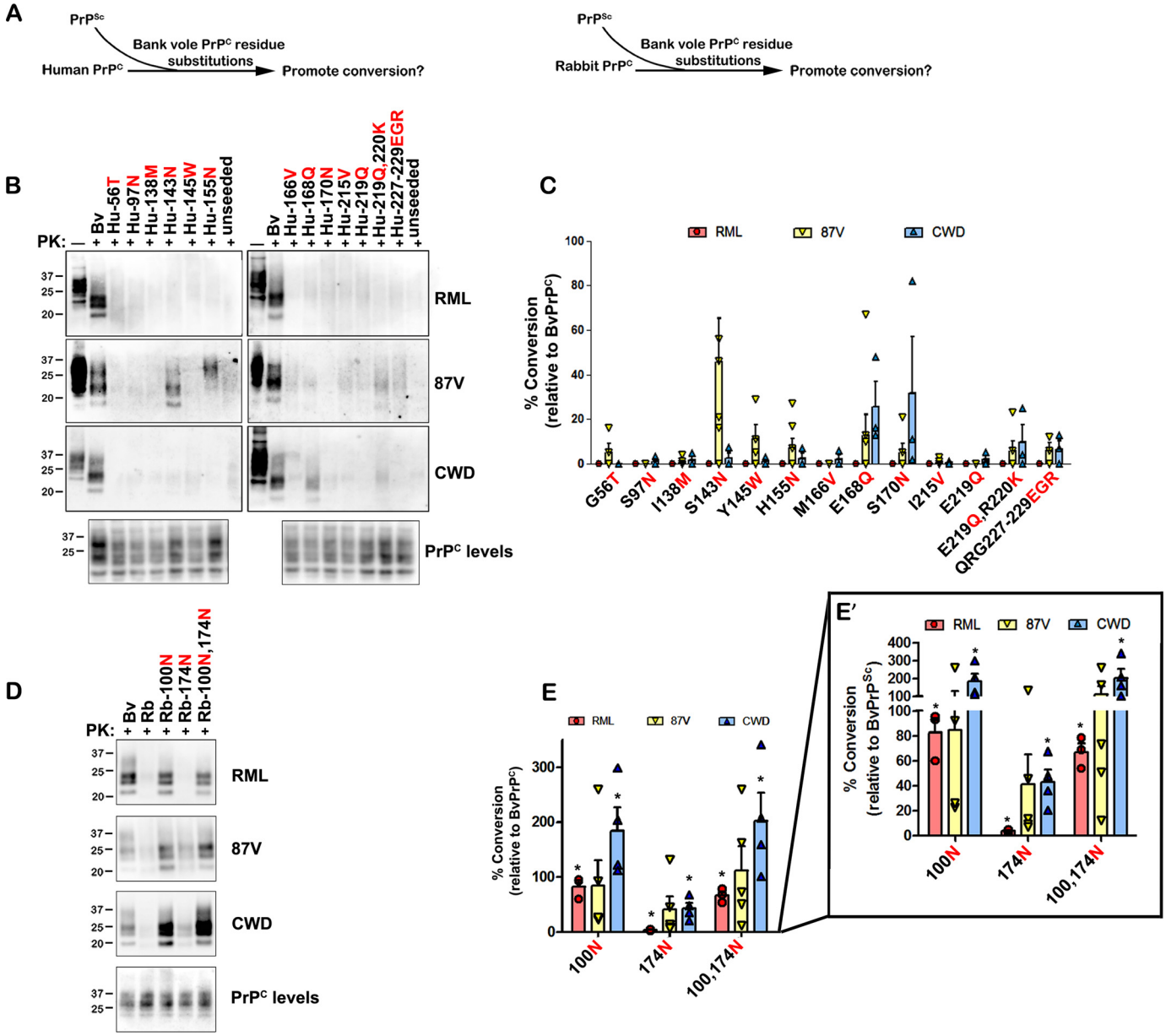

Figure 2. Key bank vole substitutions enable conversion of human and rabbit PrP^C. *A*, schematic for experimental approach. HuPrP^C or RbPrP^C with BvPrP^C substitutions was seeded with mouse or elk prions, and the newly converted PrP^{Sc} was measured after 24 h. *B*, representative immunoblots show the impact of single BvPrP^C substitutions on conversion of HuPrP^C by RML, 87V, or CWD prions. *C*, quantitative analysis shows that the S143N, E168Q, and S170N substitutions promote conversion of HuPrP^C for certain PrP^{Sc} seeds. *D*, representative immunoblots show the conversion of RbPrP^C with the G100N, S174N, or G100N,S174N substitutions. *E*, quantitative analysis shows that the G100N and G100N,S174N promote conversion of RbPrP^C. *E′* shows the quantified data with a segmented *y* axis. Quantified data in *C* and *E* are from three to seven or three to five independent experiments, respectively. Standard *error bars* indicate the observed variance. *, $p < 0.05$, one-sample *t* test. One-way ANOVA with Tukey post hoc test revealed statistically significant differences between the following residues: for *C*, for 87V between residue 143 and residue 56, 155, 170, 219, and 219/220 (*, $p < 0.05$), as well as between residue 143 and residues 97, 138, 166, and 215 (**, $p < 0.01$); for *E*, for RML between residue 100 or 174 and 100/174 (***, $p < 0.001$), and for CWD, between residue 100 or 100/174 and 174 (*, $p < 0.01$).

plete bank vole β2–α2 loop sequence (M166V, E168Q, and S170N substitutions) was converted by CWD prions as efficiently as bank vole PrP^C; no additional bank vole substitutions further enhanced conversion (Fig. 3, *A* and *B*). These results indicate that the bank vole β2–α2 loop sequence is necessary and sufficient for elk CWD cross-seeding of HuPrP^C.

In contrast to elk CWD, mouse prions RML and 87V minimally converted HuPrP^C containing the bank vole β2–α2 loop sequence (<15%; Fig. 3, *A* and *B*). Because the N143S substitution in the β1–α1 loop had inhibited BvPrP conversion (Fig. 1*E*), we next tested whether HuPrP^C with the bank vole β1–α1 and β2–α2 loop segments (S143N, Y145W, M166V, E168Q, and S170N) would be converted by mouse prions. These five-residue exchanges, which add three more Asn/Gln residues to the human sequence and remove a charged residue, led to substantially higher levels of HuPrP^C conversion by 87V prions (101%), but not by RML prions (8%) (Fig. 3, *C* and *D*). These results indicate that in two critical segments known to form steric zippers, the β1–α1 loop (positions 143–145) (36) and the β2–α2 loop (positions 166–170) (14), bank vole residues enable efficient conversion of HuPrP^C seeded by mouse 87V prions. Because RML was not converted, these data also suggest that

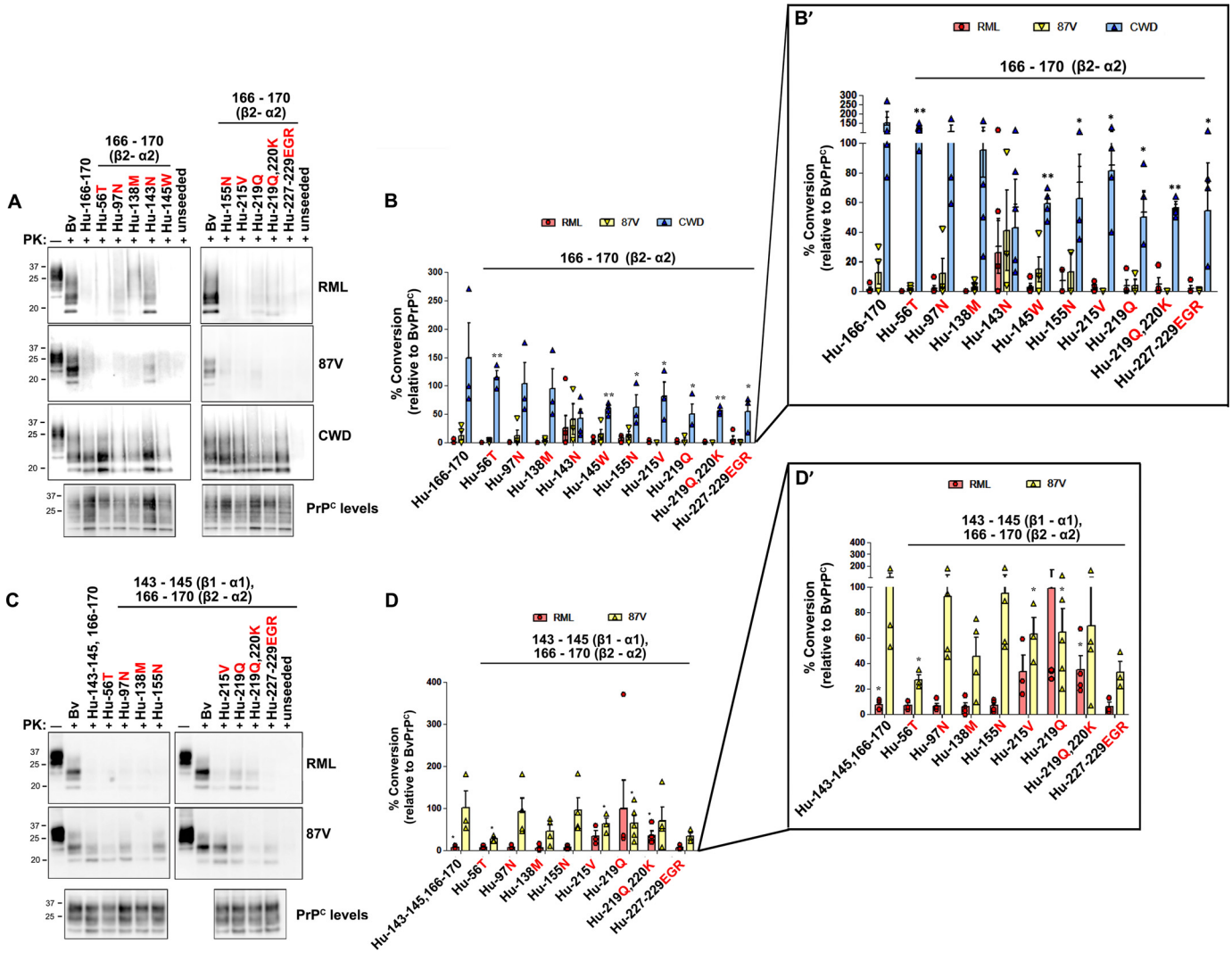

Figure 3. Bank vole substitutions in human PrP^C promote 87V or RML prion conversion. *A*, representative immunoblots demonstrate conversion of HuPrP^C with the BvPrP^C β2–α2 loop sequence together with additional BvPrP^C amino acid substitutions. *B*, quantitative analysis reveals that HuPrP^C with the BvPrP^C β2–α2 loop is converted by CWD, but not RML or 87V prions. *C*, representative immunoblots show conversion of HuPrP^C sequences containing the BvPrP^C β1–α1 and β2–α2 loop sequences. *D*, quantitative analysis indicates that HuPrP^C with the BvPrP^C β1–α1 and β2–α2 loop sequences was converted by 87V prions. Conversion by RML prions additionally required the I215V or E219Q substitution. Note that four of five measurements of Hu-Gln^{219} ranged from 28 to 35% conversion, whereas one measurement was >300. *B′* and *D′* show the quantified data with a segmented *y* axis. Quantified data in *B* and *D* are from three to five independent experiments. Standard *error bars* indicate the observed variance. *, $p < 0.05$; **, $p < 0.01$, one sample *t* test.

mouse RML and 87V prions differ in the number and location of PrP^C segments required for efficient conversion.

To identify the residues controlling conversion of HuPrP^C by RML prions, 10 additional BvPrP^C substitutions (in groups of 1–3) were incorporated into the HuPrP^C–bank vole β1–α1/β2–α2 chimera and tested for conversion. Of the 10 residues tested, RML prions only converted to >20% PrP^C having the additional I215V, E219Q, or E219Q, R220K substitutions (Fig. 3, *C* and *D*; note for Glu^{219}, four of five measurements resulted in 28–35% conversion). These experiments indicate that four Asn/Gln substitutions, which were in the β1–α1 and β2–α2 loop segments (Asn^{143}, Gln^{168}, and Asn^{170}), and the C terminus of α-helix 3 (residue 219), enable limited conversion of human PrP^C by RML. The Val^{215} substitution also enhanced conversion by RML. Interestingly, HuPrP^C with the bank vole β2–α2 loop, together with the individual substitutions S143N, I215V, or E219Q, was not converted to high levels by RML prions (Fig. 3, *A* and *B*), indicating that exchanges in all three segments were essential for conversion of HuPrP^C by RML prions.

Prion conversion enhanced by Asn/Gln substitutions is highly position- and side chain-dependent

Strikingly, five of five single substitutions that inhibit conversion of BvPrP^C to less than 20% or that promote conversion of HuPrP^C and RbPrP^C to greater than 20% involved the loss or gain of Asn/Gln residues, respectively. Mammalian PrP^C from 24 species revealed 26–31 Asn/Gln residues scattered throughout the protein; bank vole PrP^C has 31 Asn/Gln residues, an unusually high number, and a notably high Asn:Gln ratio (0.94) (Tables 1 and 2). To determine whether the position of the Asn or Gln substitution within a segment impacts conversion, Asn/Gln substitutions were placed at sites flanking positions 143 and 219 in HuPrP^C. For RML and 87V prions, there was little to no conversion when the Asn^{143} substitution was transposed to

Table 1
Total number of asparagine and glutamine residues in the PrP sequence of 24 species

Species	Asn	Gln	Asn/Gln total	Asn:Gln ratio
Rodents				
Bank vole (*Myodes glareolus*)	15	16	31	0.94
Meadow vole (*Microtus pennsylvanicus*)	15	16	31	0.94
Deer mouse (*Peromyscus maniculatus bairdii*)	15	16	31	0.94
Syrian golden hamster (*Mesocricetus auratus*)	15	16	31	0.94
Chinese hamster (*Cricetulus griseus*)	15	16	31	0.94
Armenian hamster (*Cricetulus migratorius*)	14	16	30	0.88
Mouse (*Mus musculus*)	13	16	29	0.81
Primates				
Black-handed spider monkey (*Ateles geoffroyi*)	14	15	29	0.93
Common marmoset (*Callithrix jacchus*)	13	16	29	0.81
Squirrel monkey (*Saimiri sciureus*)	12	17	29	0.71
Tufted capuchin (*Sapajus apella*)	12	16	28	0.75
Macaque (*Macaca mulatta, Macaca fascicularis*)	11	16	27	0.69
Human (*Homo sapiens*)	11	15	26	0.73
Chimp (*Pan troglodytes*)	10	16	26	0.63
Ruminants				
Deer (*Odocoileus* sp.)	12	17	29	0.71
Cow (*Bos taurus*)	12	17	29	0.71
Sheep (*Ovis aries*) ARR/ARQ	12	16/17	28/29	0.71–0.75
Elk (*Cervus canadensis*)	12	16	28	0.75
Carnivores				
Cat (*Felis catus*)	12	16	28	0.75
Ferret (*Mustela putorius furo*)	11	17	28	0.65
Mink (*Neovison vison*)	11	16	27	0.69
Raccoon (*Procyon lotor*)	11	16	27	0.69
Dog (*Canis familiaris*)	11	16	27	0.69
Leporids				
Rabbit (*Oryctolagus cuniculus*)	10	18	28	0.56

Table 2
PrP residue differences between species at positions 100, 143, 168, 170, 174, and 219
Bold italic residues indicate amino acids that may confer resistance to prion conversion.

Species	100	143	168	170	174	219
Bank vole	Asn	Asn	Gln	Asn	Asn	Gln
Hamster	Asn	Asn	Gln	Asn	Asn	Gln
Elk	Asn	Asn	Gln	Asn	***Thr***	Gln
Mouse	Asn	Asn	Gln	***Ser***	Asn	Gln
Cow	Asn	Asn	Gln	***Ser***	Asn	Gln
Squirrel monkey	Asn	Asn	Gln	***Ser***	Asn	***Glu***
Macaque	***His***	Asn	Gln	***Ser***	Asn	***Glu***
Sheep	Asn	Asn	Gln/***Arg***	***Ser***	Asn	Gln
Human	Asn	***Ser***	***Glu***	***Ser***	Asn	***Glu***
Rabbit	***Gly***	Asn	Gln	***Ser***	***Ser***	Gln
Dog	***Gly***	Asn	Gln	***Ser***	Asn	Gln
Ferret	***Gly***	Asn	Gln	***Ser***	Asn	Gln
Raccoon	***Gly***	Asn	Gln	***Ser***	Asn	Gln

142, 144, or 145 (Fig. 4, *A*, *B*, and *I*) Similarly, for RML prions, there was little to no conversion when the Gln^{219} substitution was transposed to position 218, 220, or 221 (Fig. 4, *C*, *D*, and *I*); thus, the promoting effect of the Asn^{143} and Gln^{219} was highly position-dependent.

To assess the specificity of the asparagine *versus* glutamine side chain on conversion, we exchanged Asn/Gln residues at four key positions of bank vole PrP (100, 143, 170, and 219). Strikingly, position 100 required an asparagine for cross-species prion conversion, because $RbPrP^{C}$-100Q was not converted efficiently by RML, 87V, or CWD prions (9, 26, and 21%, respectively; Fig. 4, *E*, *F*, and *I*). Similarly, position 143 also required an asparagine, because glutamine did not enable conversion of $HuPrP^{C}$ by RML or 87V prions (Fig. 4, *A* and *B*). In contrast, at positions 170 and 219, asparagine and glutamine were interchangeable, because Hu-Bv PrP^{C} chimeras with 170N/170Q or Gln^{219}/219N residues were efficiently converted by CWD or RML prions, respectively (≥100%; Fig. 4, *C*, *D*, and *G*–*I*). Because Asn and Gln side chains differ by only one methylene group, our findings suggest that the promoting effect of Asn/Gln substitutions is highly dependent on side chain length in certain positions (100 and 143) but not others (170 and 219). Interestingly, although leucine is somewhat structurally similar to asparagine in volume, the Leu^{143} and Leu^{219} substitutions in Hu-Bv PrP^{C} were not converted by 87V or RML, respectively (0–1%) (Fig. 4, *A*–*D*), suggesting that the side chain hydrogen bonding of the amide in the Asn/Gln is critical to prion conversion. These results indicate that the strong promoting effect of the Asn^{100} and Asn^{143} residues on prion conversion is highly position- and side chain-dependent, requiring specifically an asparagine residue.

Discussion

Prion transmission can be exquisitely sensitive to primary sequence differences between PrP^{C} and PrP^{Sc}, because even one mismatched residue can obstruct prion conversion (37–39). Bank vole PrP^{C}, however, is extraordinarily susceptible to conversion seeded by prions from other species, despite sequence differences (19, 21, 24, 25, 35, 40–42). Here we have investigated the residues that govern cross-species prion conversion by systematically testing over 40 mutated bank vole, human, and rabbit PrP^{C} sequences seeded by three dissimilar PrP^{Sc} seed sequences. Our studies revealed five amino acid substitutions that profoundly promote or inhibit prion conversion, all of which involve the gain or loss of an asparagine or glutamine residue (positions 100, 143, 168, 174, and 219). Remarkably, substituting Asn/Gln residues into PrP conferred susceptibility to sequences that otherwise resisted conversion. The relevant positions of the Asn/Gln residues varied with the incoming prion seed, consistent with PrP^{Sc} conformation determining the critical PrP^{C}–PrP^{Sc} interaction domains. Additionally, we have also established that certain positions tolerate either an Asn or a Gln, whereas others strictly require an Asn or a Gln for prion conversion.

The addition of Asn/Gln residues resulted in a sequence match with the PrP^{Sc} seed (supplemental Fig. S1), which could explain why conversion was enhanced. However, six other substitutions led to a sequence match with the seed but did not promote conversion. Additionally, for at least two positions, 170 and 219, a mismatched polar residue also promoted conversion, indicating that the side chain structure did not require a precise match with the PrP^{Sc} seed but did require a structurally similar residue. Notably, the position of the Asn/Gln residue was also important, because there were Asn/Gln residues in positions that did not significantly impact prion conversion (S97N or H155N), even in combination with the bank vole

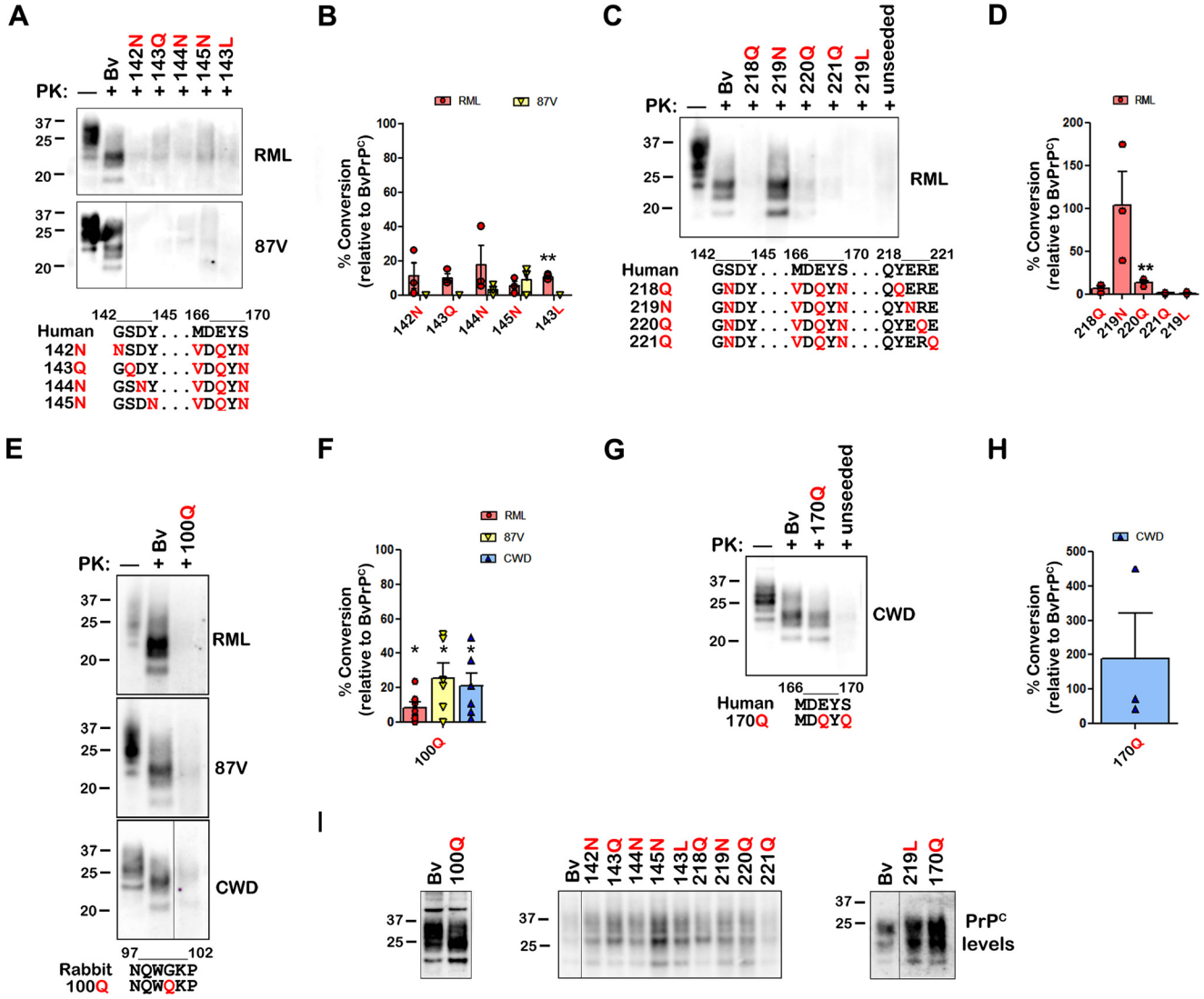

Figure 4. The impact of Asn/Gln residues on prion conversion is highly position-dependent. *A* and *B*, HuPrP^C with the BvPrP^C β2–α2 loop and the 143Q or 143L substitution is not converted by RML or 87V prions. Additionally, transposing the asparagine substitution from position 143 to flanking positions in HuPrP^C no longer promotes conversion by RML or 87V prions. *C* and *D*, HuPrP^C with the E219N, but not the E219L, substitution together with the BvPrP^C β1–α1 and β2–α2 loop sequences is efficiently converted by RML prions. Shifting the glutamine substitution from position 219 to flanking positions does not promote conversion by RML prions. *E* and *F*, RbPrP^C with the 100Q substitution was minimally converted by RML, 87V, or elk CWD prions. *G* and *H*, HuPrP^C with the Gln^{170} substitution was converted by elk CWD prions. *I*, PrP^C in lysates used for *A*–*H* show similar PrP^C levels. The blots in *A*, *E*, and *I* show single Western blots at the same exposure with intervening lanes removed for clarity. PrP^C sequence changes are shown in *red* below immunoblots. Quantified data are from three to five (*B*), three or four (*F*), or three (*H*) independent experiments. Standard *error bars* indicate the observed variance. *, $p < 0.05$; **, $p < 0.01$, one-sample *t* test. One-way ANOVA with Tukey post hoc test revealed statistically significant differences for RML between Asn^{219} and residue Asn^{218}, Asn^{220}, Asn^{221}, and Leu^{219} (*, $p < 0.05$).

β1–α1 and β2–α2 residues. Among the five key Asn/Gln residues, four residues (at positions 100, 168, 174, and 219) were located within steric zipper segments identified by the Zipper DB 3D profiling method using the seven-residue zipper (Rosetta energies below an energetic threshold of −27 kcal/mol) (Table 3), and two segments have been crystallized (positions 143 and 174) (14, 36). Taken together, these findings suggest that PrP^C–PrP^{Sc} interactions in short segments regulate prion conversion.

Prion seeding specificity is widely recognized to be controlled by one or two key residues (22, 23), for example, PrP residues 138/139 in the β1–α1 loop control seeding specificity between mouse and hamsters (38, 39) and residues 168 and 170 in the β2–α2 loop impact deer CWD–human transmission barriers (12). The mechanism underlying how residues in the β1–α1 and β2–α2 loop control conversion may be explained by microcrystal structures of the 138–143 and the 170–175 segments determined to less than 3 Å, where amino acid side chain

Table 3

Rosetta energy calculations for five steric zipper segments identified in the prion protein

The position of the N or Q residue is shown as bold text.

Asn/Gln position	Zipper segments identified by ZipperDB	Rosetta energy
		kcal/mol
100	QW**N**KPSK	−29.2
143	MIHG**N**DW	−26
168	**Q**YNNQNN	−34.6
174	QYNNQN**N**	−34.6
219	QY**Q**KESQ	−31.2

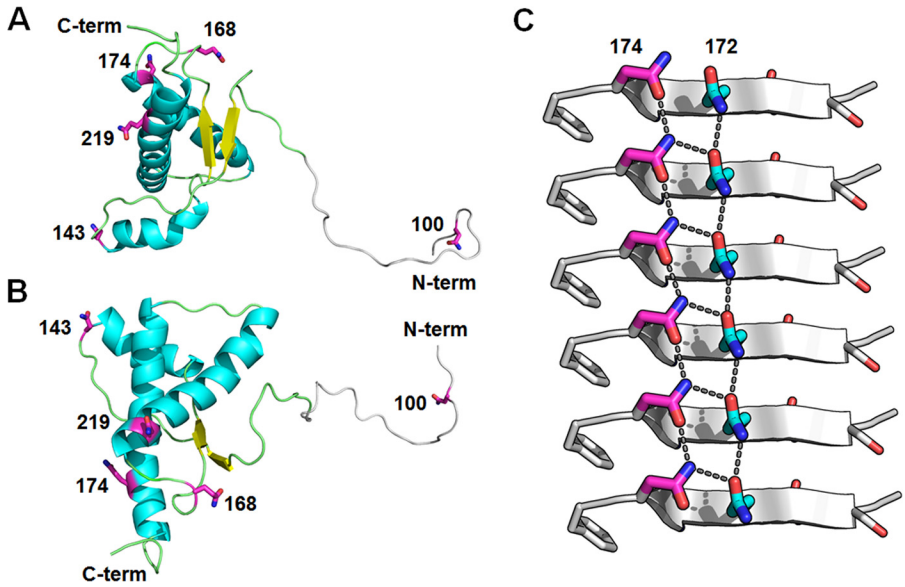

Figure 5. Proposed mechanism for prion conversion involving asparagine/glutamine residues in discrete segments of bank vole PrP^C. *A*, a ribbon diagram of the NMR BvPrP^C structure (Protein Data Bank code 2K56; Ref. 27) with critical Asn/Gln residues shown in *magenta*. The N-terminal domain of PrP^C (residues 97–118, *gray*) is modeled using Rosetta software (63). Residues 23–96 are not shown. *B*, another view of the NMR BvPrP^C structure rotated horizontally by 90°. *C*, zipper structure from PrP^{Sc} peptide (residues 170–175; Protein Data Bank code 3VFA; Ref. 36) fibril demonstrating that alignment of Asn/Gln residues along the length of the fibril axis promotes side chain hydrogen bonds in a motif known as an asparagine/glutamine-ladder. β-Strands are represented by *gray arrows*, Asm^{174} residues are shown in *magenta*, Gln^{172} residues are in *cyan*, and side chain hydrogen bonds in the asparagine/glutamine-ladder are indicated by *black dotted lines*.

differences result in microcrystals having different symmetry (14, 36). Thus, it is not entirely surprising that residue differences in these particular zipper segments had such a remarkable impact on prion transmission barriers. The surprising element here was that the residues that most profoundly impacted cross-species prion conversion were largely dominated by Asn/Gln residues.

The critical Asn/Gln residue positions for cross-species conversion differed depending on the PrP^{Sc} seed (Fig. 5), consistent with the recognized role of PrP^{Sc} conformation in prion conversion. The results using mutant PrP have enabled a partial mapping of interacting residues critical for certain prions, suggesting segments that may be exposed in PrP^{Sc}. PrP^C–PrP^{Sc} interaction at residues 215 and 219 was important for RML only, indicating that the distal C terminus is a key intermolecular contact segment for RML, but not 87V or CWD prions. Additionally, the β2–α2 loop was key for CWD-seeded conversion but insufficient for RML or 87V. Findings from our lab and others that the key interaction domains in PrP^C vary with the PrP^{Sc} conformation are consistent with those from Sup35 yeast prions, showing that short segments control prion nucleation, conformation, and species barriers (43).

How do asparagine and glutamine residues lower the energy barrier for prion cross-seeding? Of relevance to Huntington's disease, fibril assembly of the huntingtin protein is caused by expansion of poly(Q) tracts (44, 45). Perutz *et al.* (46) have proposed that Asn/Gln residues mediate protein-protein interactions in huntingtin and other Asn/Gln-rich aggregating proteins through the formation of hydrogen bond networks that stabilize β-strands, termed "polar zippers." Within a β-sheet, asparagine and glutamine residues were proposed to markedly enhance β-strand stability through intrasheet hydrogen bonds formed between both side chain and main chain amides (Fig. 5). These additional hydrogen bonds, more typically between amides of identical side chains in adjacent strands, greatly increase the stability of the β-sheet, because the parallel arrays of aligned bonds are hyperpolarized (47) and are even stronger than those in ice (48, 49). We suggest a model in which intermolecular interactions between complementary PrP segments that have a strong, hyperpolarized hydrogen bond network, such as the β2–α2 loop, stabilize newly incorporated PrP monomers onto β-sheet-rich fibrils, driving aggregation of dissimilar PrP sequences. These intermolecular contact sites may also serve as critical templating sites, directing PrP into a particular PrP^{Sc} fold. This model would be consistent with experimental findings from the β1–α1 and β2–α2 loop, where sequence differences can switch the prion conformation (11, 50, 51).

Several yeast prions, such as Ure2, Sup35, and Rnq1, contain Asn/Gln-rich domains that are required for assembly into functional prion fibrils (52, 53) and may mediate prion cross-seeding (54). The Asn/Gln residues at the N terminus of Ure2p and Sup35p play a particularly critical role in stabilizing the amyloid state (55). This Asn/Gln-rich domain is also modular, causing aggregation when introduced into other proteins (56). By comparison, mammalian prions contain one short Asn/Gln-rich domain (β2–α2 loop), with additional Asn/Gln residues interspersed throughout the protein. Thus, the Asn/Gln residues within PrP are not constrained to a single Asn/Gln-rich domain but seem to collectively promote conversion from multiple segments. Stacking of Asn/Gln residues into ladders along the length of a prion fibril would maximize interstrand hydrogen bonding and would be compatible with a parallel, in-register β-sheet structure for PrP^{Sc}.

Our studies afford insight into the mechanism of prion conversion. Asn/Gln substitutions at positions flanking Asn^{143} or Gln^{219} (positions 142, 144, 145, 218, 220, and 221) had little

effect on conversion of HuPrP^C. This finding indicates that the precise Asn/Gln position within the segment was critical for prion conversion, which is consistent with steric zipper formation at segment 138–143. For instance, Gly^{142} is located at a tight turn in the crystal structure of the 138–143 segment (36). Asn/Gln substitutions at this position would be predicted to clash with zipper formation and thus hinder prion conversion. Additionally, other substitutions in HuPrP^C that increase total Asn/Gln content, such as S97N or H155N, did not strongly promote conversion, supporting the importance of the specific position of the Asn/Gln residue in facilitating prion conversion.

Were asparagine and glutamine residues in the key positions interchangeable? PrP positions 100 and 143 required an asparagine and not a glutamine for conversion, indicating that a specific side chain length was crucial in certain positions (Fig. 5). On the other hand, positions 170 and 219 tolerated either an asparagine or glutamine; however, leucine substitutions at position 143 or 219 blocked conversion. Together, these findings underscore the importance of the hydrogen bond stabilizing ladder provided by the asparagine or glutamine side chain. In Sup35 yeast prions, asparagine residues enhance prion formation more than glutamine residues (57). Asparagine side chains are also critical for islet amyloid polypeptide fibril assembly (58).

The bank vole PrP^C sequence contains 31 Asn/Gln residues, more than most other mammals assessed here (Table 1). In comparing the Asn/Gln ratio across species, an interesting trend emerges. The species that are highly susceptible to diverse prions, such as the bank vole, have an extraordinarily high Asn/Gln ratio (0.94 in bank vole *versus* 0.56 in rabbit PrP^C), and a particularly dense stretch of Asn residues in the $\beta2$–$\alpha2$ loop. The $\beta2$–$\alpha2$ loop (QYNNQNN) is a segment suspected to be involved early in PrP nucleation and is favored by asparagine residues (59, 60). Our studies suggest that the high number of key interspersed Asn/Gln residues (Table 2) may stabilize nascent β-strands through a hydrogen bond ladder and may explain the elevated promiscuity of bank voles to cross-species prion conversion, as well as the spontaneous assembly of BvPrP^C in transgenic mice (61).

These findings argue that certain interspersed asparagine and glutamine residues may facilitate the anchoring of PrP^C to PrP^{Sc} through strengthening a replicative interface, driving prion conversion between dissimilar sequences and lowering the barrier for aggregation. Identifying the key prion segments and specific residue interactions in early stages of conversion may facilitate predictions of cross-species prion transmission. We expect that the importance of interspersed asparagine and glutamine residues in protein aggregation may be a more general phenomena applicable to other amyloidogenic proteins and may present target segments for rational therapeutic design.

Experimental procedures

Cell-lysate protein misfolding cyclic amplification

The pcDNA3.1 vector (Invitrogen) with the mouse, human, bank vole, or rabbit *Prnp* encoding the 3F4 epitope (Met^{109} and Met^{112} human numbering) was used as a template for site-directed mutagenesis (QuikChange site-directed mutagenesis kit; Agilent). PrP-deficient RK13 cells (ATCC) were transfected with 5–10 μg of plasmid DNA using Lipofectamine 3000 (Invitrogen). At 24 h post-transfection, the cells were washed twice in PBS, harvested in 1 ml of PBS, and centrifuged for 1 min at 1,000 $\times$ *g*. The pellet was resuspended in PMCA buffer (PBS containing 1% Triton X-100, 150 mM NaCl, and 5 mM EDTA plus Complete^{TM} protease inhibitors), passed repeatedly through a 27-gauge needle, and clarified by centrifuging at 2,000 $\times$ *g* for 1 min.

RML prions from C57BL/6 mice (*Prnp* encoding Leu^{109}, Thr^{189}, human numbering), 87V prions from VM/DK mice (*Prnp* encoding Phe^{109} and Val^{189}), and CWD prions from elk (Met^{129}) were used to seed human, bank vole, and rabbit PrP^C (*Prnp* sequences shown in Fig. 1 and supplemental Fig. S1). The PrP^C was newly prepared for each independent experiment. The prion seeds were derived from brain homogenate that was pooled from mice inoculated with the same prion strain or from naturally infected elk. The brain homogenate samples pooled to generate the seeds were consistent between the experiments. Prion-infected brain homogenate (10% w/v) was added into PrP^C-expressing RK13 cell lysate (1:10, PrP^{Sc}:PrP^C by volume) and subjected to repeated 5-s sonication pulses (S4000, QSonica) with 10 min of incubation between each pulse over a total period of 24 h. Sonication power was maintained at 50–60%, and samples were continuously rotated in a water bath at 37 °C. Samples were then digested with 200 μg/ml PK for 30 min at 37 °C and analyzed by Western blot using the anti-PrP monoclonal antibody 3F4 (62). PrP^C levels were measured by blotting 1–2 μl from unseeded lysates. Signals were quantified using a Fujifilm LAS-4000 imager and multi-gauge software and compared by the percentage of conversion compared with control samples (considered 100%). PK-digested unseeded lysates were included in all experiments to exclude PrP^{Sc} contamination of the PMCA substrates and spontaneous assembly of mutant PrP^C protein. At least three independent experimental replicates were performed for each mutant and each prion strain used as seed.

Statistical analysis

One-way ANOVA with Tukey post hoc test and a one-sample *t* test were used to analyze the conversion data from each mutant PrP. For the one-sample *t* test, the conversion of human or rabbit substitutions in bank vole PrP^C was compared against a mean of 100 (null hypothesis) to assess whether the mutation(s) inhibited PrP conversion. The conversion of bank vole substitutions in human or rabbit PrP^C was compared against a mean of 0 to assess whether the mutation(s) promoted PrP conversion.

Author contributions—T. D. K. and C. J. S. designed the study and wrote the paper. T. D. K. and P. A.-C. performed the experiments, and N. A. provided technical assistance. T. D. K., P. A.-C., L. J., J. A. R., D. S. E., and C. J. S. analyzed the experiments. All authors reviewed the results and approved the final version of the manuscript.

Acknowledgment—We thank Dr. Steven Edland for discussion of the statistical analyses.

References

1. Prusiner, S. B. (1982) Novel proteinaceous infectious particles cause scrapie. *Science* **216,** 136–144
2. Jarrett, J. T., and Lansbury, P. T., Jr. (1993) Seeding "one-dimensional crystallization" of amyloid: a pathogenic mechanism in Alzheimer's disease and scrapie? *Cell* **73,** 1055–1058
3. Krotee, P., Rodriguez, J. A., Sawaya, M. R., Cascio, D., Reyes, F. E., Shi, D., Hattne, J., Nannenga, B. L., Oskarsson, M. E., Philipp, S., Griner, S., Jiang, L., Glabe, C. G., Westermark, G. T., Gonen, T., *et al.* (2017) Atomic structures of fibrillar segments of hIAPP suggest tightly mated β-sheets are important for cytotoxicity. *eLife* **6,** e19273b
4. Clouscard, C., Beaudry, P., Elsen, J. M., Milan, D., Dussaucy, M., Bounneau, C., Schelcher, F., Chatelain, J., Launay, J. M., and Laplanche, J. L. (1995) Different allelic effects of the codons 136 and 171 of the prion protein gene in sheep with natural scrapie. *J. Gen. Virol.* **76,** 2097–2101
5. Asante, E. A., Smidak, M., Grimshaw, A., Houghton, R., Tomlinson, A., Jeelani, A., Jakubcova, T., Hamdan, S., Richard-Londt, A., Linehan, J. M., Brandner, S., Alpers, M., Whitfield, J., Mead, S., Wadsworth, J. D., *et al.* (2015) A naturally occurring variant of the human prion protein completely prevents prion disease. *Nature* **522,** 478–481
6. Priola, S. A., Chabry, J., and Chan, K. (2001) Efficient conversion of normal prion protein (PrP) by abnormal hamster PrP is determined by homology at amino acid residue 155. *J. Virol.* **75,** 4673–4680
7. Bruce, M. E., Will, R. G., Ironside, J. W., McConnell, I., Drummond, D., Suttie, A., McCardle, L., Chree, A., Hope, J., Birkett, C., Cousens, S., Fraser, H., and Bostock, C. J. (1997) Transmissions to mice indicate that "new variant" CJD is caused by the BSE agent. *Nature* **389,** 498–501
8. Kirkwood, J. K., and Cunningham, A. A. (1994) Epidemiological observations on spongiform encephalopathies in captive wild animals in the British Isles. *Vet. Rec.* **135,** 296–303
9. Haire, L. F., Whyte, S. M., Vasisht, N., Gill, A. C., Verma, C., Dodson, E. J., Dodson, G. G., and Bayley, P. M. (2004) The crystal structure of the globular domain of sheep prion protein. *J. Mol. Biol.* **336,** 1175–1183
10. Riek, R., Hornemann, S., Wider, G., Billeter, M., Glockshuber, R., and Wüthrich, K. (1996) NMR structure of the mouse prion protein domain PrP (121–231). *Nature* **382,** 180–182
11. Sigurdson, C. J., Nilsson, K. P., Hornemann, S., Manco, G., Fernández-Borges, N., Schwarz, P., Castilla, J., Wüthrich, K., and Aguzzi, A. (2010) A molecular switch controls interspecies prion disease transmission in mice. *J. Clin. Invest.* **120,** 2590–2599
12. Kurt, T. D., Jiang, L., Fernández-Borges, N., Bett, C., Liu, J., Yang, T., Spraker, T. R., Castilla, J., Eisenberg, D., Kong, Q., and Sigurdson, C. J. (2015) Human prion protein sequence elements impede cross-species chronic wasting disease transmission. *J. Clin. Invest.* **125,** 1485–1496
13. Kurt, T. D., Jiang, L., Bett, C., Eisenberg, D., and Sigurdson, C. J. (2014) A proposed mechanism for the promotion of prion conversion involving a strictly conserved tyrosine residue in the β2–α2 loop of PrP^C. *J. Biol. Chem.* **289,** 10660–10667
14. Sawaya, M. R., Sambashivan, S., Nelson, R., Ivanova, M. I., Sievers, S. A., Apostol, M. I., Thompson, M. J., Balbirnie, M., Wiltzius, J. J., McFarlane, H. T., Madsen, A. Ø., Riekel, C., and Eisenberg, D. (2007) Atomic structures of amyloid cross-beta spines reveal varied steric zippers. *Nature* **447,** 453–457
15. Gazit, E. (2002) A possible role for pi-stacking in the self-assembly of amyloid fibrils. *FASEB J.* **16,** 77–83
16. Eisenberg, D. S., and Sawaya, M. R. (2017) Structural studies of amyloid proteins at the molecular level. *Annu. Rev. Biochem.* **86,** 69–95
17. Chandler, R. L. (1971) Experimental transmission of scrapie to voles and Chinese hamsters. *Lancet* **1,** 232–233
18. Nonno, R., Di Bari, M. A., Cardone, F., Vaccari, G., Fazzi, P., Dell'Omo, G., Cartoni, C., Ingrosso, L., Boyle, A., Galeno, R., Sbriccoli, M., Lipp, H. P., Bruce, M., Pocchiari, M., and Agrimi, U. (2006) Efficient transmission and characterization of Creutzfeldt–Jakob disease strains in bank voles. *PLoS Pathog.* **2,** e12
19. Di Bari, M. A., Chianini, F., Vaccari, G., Esposito, E., Conte, M., Eaton, S. L., Hamilton, S., Finlayson, J., Steele, P. J., Dagleish, M. P., Reid, H. W., Bruce, M., Jeffrey, M., Agrimi, U., and Nonno, R. (2008) The bank vole (*Myodes glareolus*) as a sensitive bioassay for sheep scrapie. *J. Gen. Virol.* **89,** 2975–2985
20. Heisey, D. M., Mickelsen, N. A., Schneider, J. R., Johnson, C. J., Johnson, C. J., Langenberg, J. A., Bochsler, P. N., Keane, D. P., and Barr, D. J. (2010) Chronic wasting disease (CWD) susceptibility of several North American rodents that are sympatric with cervid CWD epidemics. *J. Virol.* **84,** 210–215
21. Di Bari, M. A., Nonno, R., Castilla, J., D'Agostino, C., Pirisinu, L., Riccardi, G., Conte, M., Richt, J., Kunkle, R., Langeveld, J., Vaccari, G., and Agrimi, U. (2013) Chronic wasting disease in bank voles: characterisation of the shortest incubation time model for prion diseases. *PLoS Pathog.* **9,** e1003219
22. Vorberg, I., Groschup, M. H., Pfaff, E., and Priola, S. A. (2003) Multiple amino acid residues within the rabbit prion protein inhibit formation of its abnormal isoform. *J. Virol.* **77,** 2003–2009
23. Agrimi, U., Nonno, R., Dell'Omo, G., Di Bari, M. A., Conte, M., Chiappini, B., Esposito, E., Di Guardo, G., Windl, O., Vaccari, G., and Lipp, H. P. (2008) Prion protein amino acid determinants of differential susceptibility and molecular feature of prion strains in mice and voles. *PLoS Pathog.* **4,** e1000113
24. Espinosa, J. C., Nonno, R., Di Bari, M., Aguilar-Calvo, P., Pirisinu, L., Fernández-Borges, N., Vanni, I., Vaccari, G., Marín-Moreno, A., Frassanito, P., Lorenzo, P., Agrimi, U., and Torres, J. M. (2016) PrP^C governs susceptibility to prion strains in bank vole, while other host factors modulate strain features. *J. Virol.* **90,** 10660–10669
25. Piening, N., Nonno, R., Di Bari, M., Walter, S., Windl, O., Agrimi, U., Kretzschmar, H. A., and Bertsch, U. (2006) Conversion efficiency of bank vole prion protein *in vitro* is determined by residues 155 and 170, but does not correlate with the high susceptibility of bank voles to sheep scrapie in vivo. *J. Biol. Chem.* **281,** 9373–9384
26. Mays, C. E., Yeom, J., Kang, H. E., Bian, J., Khaychuk, V., Kim, Y., Bartz, J. C., Telling, G. C., and Ryou, C. (2011) *In vitro* amplification of misfolded prion protein using lysate of cultured cells. *PLoS One* **6,** e18047
27. Christen, B., Pérez, D. R., Hornemann, S., and Wüthrich, K. (2008) NMR structure of the bank vole prion protein at 20 degrees C contains a structured loop of residues 165–171. *J. Mol. Biol.* **383,** 306–312
28. Zahn, R., Liu, A., Lührs, T., Riek, R., von Schroetter, C., López García, F., Billeter, M., Calzolai, L., Wider, G., and Wüthrich, K. (2000) NMR solution structure of the human prion protein. *Proc. Natl. Acad. Sci. U.S.A.* **97,** 145–150
29. Wen, Y., Li, J., Yao, W., Xiong, M., Hong, J., Peng, Y., Xiao, G., and Lin, D. (2010) Unique structural characteristics of the rabbit prion protein. *J. Biol. Chem.* **285,** 31682–31693
30. Bett, C., Joshi-Barr, S., Lucero, M., Trejo, M., Liberski, P., Kelly, J. W., Masliah, E., and Sigurdson, C. J. (2012) Biochemical properties of highly neuroinvasive prion strains. *PLoS Pathog.* **8,** e1002522
31. Lund, C., Olsen, C. M., Tveit, H., and Tranulis, M. A. (2007) Characterization of the prion protein 3F4 epitope and its use as a molecular tag. *J. Neurosci. Methods* **165,** 183–190
32. Barlow, R. M., and Rennie, J. C. (1976) The fate of ME7 scrapie infection in rats, guinea-pigs and rabbits. *Res. Vet. Sci.* **21,** 110–111
33. Gibbs, C. J., Jr., and Gajdusek, D. C. (1973) Experimental subacute spongiform virus encephalopathies in primates and other laboratory animals. *Science* **182,** 67–68
34. Raymond, G. J., Bossers, A., Raymond, L. D., O'Rourke, K. I., McHolland, L. E., Bryant, P. K., 3rd, Miller, M. W., Williams, E. S., Smits, M., and Caughey, B. (2000) Evidence of a molecular barrier limiting susceptibility of humans, cattle and sheep to chronic wasting disease. *EMBO J.* **19,** 4425–4430
35. Watts, J. C., Giles, K., Patel, S., Oehler, A., DeArmond, S. J., and Prusiner, S. B. (2014) Evidence that bank vole PrP is a universal acceptor for prions. *PLoS Pathog.* **10,** e1003990
36. Apostol, M. I., Wiltzius, J. J., Sawaya, M. R., Cascio, D., and Eisenberg, D. (2011) Atomic structures suggest determinants of transmission barriers in mammalian prion disease. *Biochemistry* **50,** 2456–2463
37. Collinge, J. (2016) Mammalian prions and their wider relevance in neurodegenerative diseases. *Nature* **539,** 217–226

38. Priola, S. A., and Chesebro, B. (1995) A single hamster PrP amino acid blocks conversion to protease-resistant PrP in scrapie-infected mouse neuroblastoma cells. *J. Virol.* **69,** 7754–7758
39. Vanik, D. L., Surewicz, K. A., and Surewicz, W. K. (2004) Molecular basis of barriers for interspecies transmissibility of mammalian prions. *Mol. Cell* **14,** 139–145
40. Orrú, C. D., Groveman, B. R., Raymond, L. D., Hughson, A. G., Nonno, R., Zou, W., Ghetti, B., Gambetti, P., and Caughey, B. (2015) Bank vole prion protein as an apparently universal substrate for RT-QuIC-based detection and discrimination of prion strains. *PLoS Pathog.* **11,** e1004983
41. Pirisinu, L., Di Bari, M. A., D'Agostino, C., Marcon, S., Riccardi, G., Poleggi, A., Cohen, M. L., Appleby, B. S., Gambetti, P., Ghetti, B., Agrimi, U., and Nonno, R. (2016) Gerstmann–Straussler–Scheinker disease subtypes efficiently transmit in bank voles as genuine prion diseases. *Sci. Rep.* **6,** 20443
42. Nonno, R., Di Bari, M. A., Cardone, F., Vaccari, G., Fazzi, P., Dell'Omo, G., Cartoni, C., Ingrosso, L., Boyle, A., Galeno, R., Sbriccoli, M., Lipp, H. P., Bruce, M., Pocchiari, M., and Agrimi, U. (2006) Efficient transmission and characterization of Creutzfeldt–Jakob disease strains in bank voles. *PLoS Pathog.* **2,** e12
43. Tessier, P. M., and Lindquist, S. (2007) Prion recognition elements govern nucleation, strain specificity and species barriers. *Nature* **447,** 556–561
44. Scherzinger, E., Lurz, R., Turmaine, M., Mangiarini, L., Hollenbach, B., Hasenbank, R., Bates, G. P., Davies, S. W., Lehrach, H., and Wanker, E. E. (1997) Huntingtin-encoded polyglutamine expansions form amyloid-like protein aggregates *in vitro* and *in vivo*. *Cell* **90,** 549–558
45. Scherzinger, E., Sittler, A., Schweiger, K., Heiser, V., Lurz, R., Hasenbank, R., Bates, G. P., Lehrach, H., and Wanker, E. E. (1999) Self-assembly of polyglutamine-containing huntingtin fragments into amyloid-like fibrils: implications for Huntington's disease pathology. *Proc. Natl. Acad. Sci. U.S.A.* **96,** 4604–4609
46. Perutz, M. F., Johnson, T., Suzuki, M., and Finch, J. T. (1994) Glutamine repeats as polar zippers: their possible role in inherited neurodegenerative diseases. *Proc. Natl. Acad. Sci. U.S.A.* **91,** 5355–5358
47. Mompeán, M., Nogales, A., Ezquerra, T. A., and Laurents, D. V. (2016) Complex system assembly underlies a two-tiered model of highly delocalized electrons. *J. Phys. Chem. Lett.* **7,** 1859–1864
48. Tsemekhman, K., Goldschmidt, L., Eisenberg, D., and Baker, D. (2007) Cooperative hydrogen bonding in amyloid formation. *Protein Sci.* **16,** 761–764
49. Eisenberg, D., and Jucker, M. (2012) The amyloid state of proteins in human diseases. *Cell* **148,** 1188–1203
50. Bett, C., Fernández-Borges, N., Kurt, T. D., Lucero, M., Nilsson, K. P., Castilla, J., and Sigurdson, C. J. (2012) Structure of the β2–α2 loop and interspecies prion transmission. *FASEB J.* **26,** 2868–2876
51. Jones, E. M., and Surewicz, W. K. (2005) Fibril conformation as the basis of species- and strain-dependent seeding specificity of mammalian prion amyloids. *Cell* **121,** 63–72
52. Serio, T. R., and Lindquist, S. L. (1999) [PSI+]: an epigenetic modulator of translation termination efficiency. *Annu. Rev. Cell Dev. Biol.* **15,** 661–703
53. Wickner, R. B., Taylor, K. L., Edskes, H. K., Maddelein, M. L., Moriyama, H., and Roberts, B. T. (1999) Prions in *Saccharomyces* and *Podospora* spp.: protein-based inheritance. *Microbiol. Mol. Biol. Rev.* **63,** 844–861
54. Osherovich, L. Z., and Weissman, J. S. (2001) Multiple Gln/Asn-rich prion domains confer susceptibility to induction of the yeast [PSI$^+$] prion. *Cell* **106,** 183–194
55. DePace, A. H., Santoso, A., Hillner, P., and Weissman, J. S. (1998) A critical role for amino-terminal glutamine/asparagine repeats in the formation and propagation of a yeast prion. *Cell* **93,** 1241–1252
56. Wickner, R. B., Taylor, K. L., Edskes, H. K., and Maddelein, M. L. (2000) Prions: portable prion domains. *Curr. Biol.* **10,** R335–R337
57. Halfmann, R., Alberti, S., Krishnan, R., Lyle, N., O'Donnell, C. W., King, O. D., Berger, B., Pappu, R. V., and Lindquist, S. (2011) Opposing effects of glutamine and asparagine govern prion formation by intrinsically disordered proteins. *Mol. Cell* **43,** 72–84
58. Koo, B. W., Hebda, J. A., and Miranker, A. D. (2008) Amide inequivalence in the fibrillar assembly of islet amyloid polypeptide. *Protein Eng. Des. Sel.* **21,** 147–154
59. Avbelj, M., Hafner-Bratkovič, I., and Jerala, R. (2011) Introduction of glutamines into the B2-H2 loop promotes prion protein conversion. *Biochem. Biophys. Res. Commun.* **413,** 521–526
60. Reddy, G., Straub, J. E., and Thirumalai, D. (2009) Dynamics of locking of peptides onto growing amyloid fibrils. *Proc. Natl. Acad. Sci. U.S.A.* **106,** 11948–11953
61. Watts, J. C., Giles, K., Stöhr, J., Oehler, A., Bhardwaj, S., Grillo, S. K., Patel, S., DeArmond, S. J., and Prusiner, S. B. (2012) Spontaneous generation of rapidly transmissible prions in transgenic mice expressing wild-type bank vole prion protein. *Proc. Natl. Acad. Sci. U.S.A.* **109,** 3498–3503
62. Kascsak, R. J., Rubenstein, R., Merz, P. A., Tonna-DeMasi, M., Fersko, R., Carp, R. I., Wisniewski, H. M., and Diringer, H. (1987) Mouse polyclonal and monoclonal antibody to scrapie-associated fibril proteins. *J. Virol.* **61,** 3688–3693
63. Bradley, P., Misura, K. M., and Baker, D. (2005) Toward high-resolution *de novo* structure prediction for small proteins. *Science* **309,** 1868–1871

Asparagine and glutamine ladders promote cross-species prion conversion

Timothy D. Kurt, Patricia Aguilar-Calvo, Lin Jiang, José A. Rodriguez, Nazilla Alderson, David S. Eisenberg and Christina J. Sigurdson

J. Biol. Chem. 2017, 292:19076-19086.
doi: 10.1074/jbc.M117.794107 originally published online September 20, 2017